ELSEVIER

Journal of Alloys and Compounds 444–445 (2007) 429–433

Journal of ALLOYS AND COMPOUNDS

www.elsevier.com/locate/jallcom

Ion beam irradiation of U-, Th- and Ce-doped pyrochlores

J. Lian [a], S.V. Yudintsev [b], S.V. Stefanovsky [c], L.M. Wang [d], R.C. Ewing [a,d,*]

[a] *Department of Geological Sciences, University of Michigan, Ann Arbor, MI 48109-1005, USA*
[b] *Institute of Geology of Ore Deposits RAS, Moscow 109017, Russia*
[c] *SIA Radon, Moscow 119121, Russia*
[d] *Department of Nuclear Engineering & Radiological Sciences, University of Michigan, Ann Arbor, MI 48109, USA*

Received 21 June 2006; received in revised form 21 October 2006; accepted 30 October 2006
Available online 28 November 2006

Abstract

U-, Th- and Ce-doped pyrochlores were synthesized by solid state reaction: $(Ca_{0.62}Gd_{0.97}U_{0.23})(Zr_{0.84}Ti_{1.34})O_{6.9}$, $(Ca_{0.47}Gd_{0.95}Th_{0.40})(Zr_{1.29}Ti_{0.89})O_{7.05}$, $(Ca_{0.44}GdTh_{0.42})Zr_{2.13}O_{7.05}$, $Ca_{0.91}Th_{0.84}Zr_{2.25}O_{7.09}$ and $Ca_{1.04}Ce_{0.97}Ti_{1.99}O_{6.96}$. Their response to the radiation damage from the recoils of the alpha-decay events has been simulated by 1 MeV Kr^{2+} ion irradiation and studied by *in situ* transmission electron microscopy (TEM). An ion beam-induced pyrochlore-to-fluorite structural transition occurred for all compositions, and independent kinetics were observed for cation and anion disordering processes. Similar to the stoichiometric titanate and zirconate pyrochlores, the Ti-rich compositions are susceptible to ion beam-induced amorphization; while, the Zr-rich compositions are more radiation "resistant". A close relation between the critical amorphization temperature of the U-, Th- and Ce-doped pyrochlores and the average cation ionic radius ratio of the A- and B-sites was observed.

Keywords: Radiation effects; Nuclear waste forms; Pyrochlores; Ion irradiation

1. Introduction

The design and selection of actinide-bearing materials for nuclear waste forms for the safe disposition of Pu and the "minor" actinides (e.g., Np, Am, Cm) generated by the nuclear fuel cycle is critical for the development of next generation of nuclear power reactors. Isometric pyrochlores, $A_2B_2O_7$, have been proposed as potential hosts for the immobilization of actinides, particularly Pu, due to their chemical durability and their ability to accommodate a wide variety of waste stream compositions [1–7]. The self-irradiation effects from the α-decay events of the incorporated actinides in the transplutonium-zirconate pyrochlores $An_2Zr_2O_7$ (An = Am, Cf) have recently been reported [8]. Ion beam irradiation has been widely used to simulate the ballistic effects of α-decay damage from the incorporated actinides for different pyrochlore compositions [9–15], and a synthetic $Gd_2Ti_2O_7$ doped with a short-lived actinide ^{244}Cm (half-life = 18.1 years) shows a similar response behavior to α-decay damage and ion beam irradiation [3,16]. In this paper, the response behaviors of Ce-, U- and Th-doped pyrochlores to radiation damage were investigated by 1 MeV Kr^{2+} irradiation. The microstructural evolution upon ion beam irradiation has been characterized in detail by *in situ* transmission electron microscopy (TEM) and *ex situ* high-resolution TEM observation.

2. Experimental

The actinide-doped pyrochlores were synthesized with designed compositions of: $CaCeTi_2O_7$, $(Ca_{0.5}GdTh_{0.5})(ZrTi)O_7$, $(Ca_{0.5}GdTh_{0.5})Zr_2O_7$, $CaThZr_2O_7$, and $(Ca_{0.5}GdU_{0.5})(ZrTi)O_7$. These samples were prepared by pressing and sintering a mixture of CeO_2, UO_2 or ThO_2, TiO_2, ZrO_2, and Gd_2O_3 as a neutron absorber, as well as a certain amount of CaO for charge compensation, at 1775–1825 K for 6–10 h in air. The Ce-doped sample was sintered at 1575–1625 K for 5–50 h in pure oxygen [17]. The Ce-doped sample is composed mainly of pyrochlore, residual CeO_2 and perovskite. In the U- and Th-doped samples, the dominant phase is pyrochlore, with minor, residual phases of (U, Zr)O_2 or ThO_2. Based on quantitative analysis by energy dispersive spectroscopy (EDS) measurements during scanning electron microscopy observation, the actual stoichiometries of the corresponding pyrochlore phases were determined to be: $Ca_{1.04}Ce_{0.97}Ti_{1.99}O_{6.96}$, $(Ca_{0.47}Gd_{0.95}Th_{0.40})(Zr_{1.29}Ti_{0.89})O_{7.05}$, $(Ca_{0.44}GdTh_{0.42})Zr_{2.13}O_{7.05}$, $Ca_{0.91}Th_{0.84}Zr_{2.25}O_{7.09}$ and $Ca_{0.62}Gd_{0.97}U_{0.23})(Zr_{0.84}Ti_{1.34})O_{6.90}$, respectively.

A 1 MeV Kr^{2+} ion irradiation was performed using the IVEM-Tandem Facility at the Argonne National Laboratory over the temperature range from

* Corresponding author. Tel.: +1 734 763 9295; fax: +1 734 647 5706.
E-mail address: rodewing@umich.edu (R.C. Ewing).

0925-8388/$ – see front matter © 2006 Elsevier B.V. All rights reserved.
doi:10.1016/j.jallcom.2006.10.133

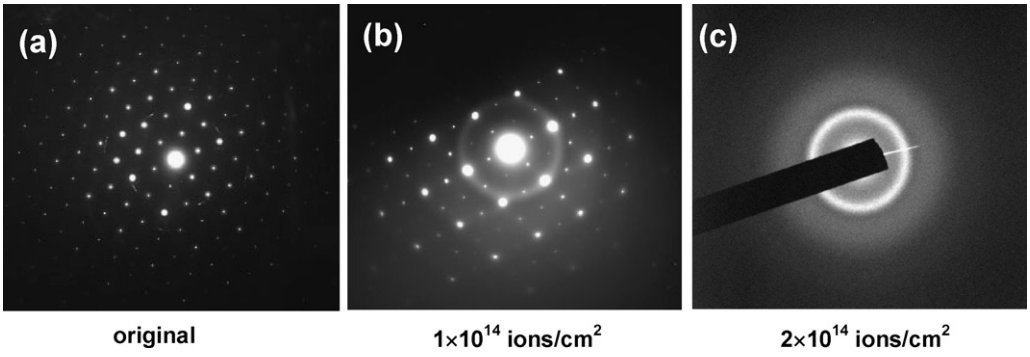

Fig. 1. A sequence of SAED patterns for $Ca_{1.04}Ce_{0.97}Ti_{1.99}O_7$ irradiated by 1 MeV Kr^{2+} at room temperature at different ion fluences: (a) original; (b) 1×10^{14} ions/cm^2; (c) 2×10^{14} ions/cm^2.

293 to 1173 K. During irradiation, the ion beam was aligned approximately normal to the sample surface. The ion flux was 6.25×10^{11} cm^{-2} s^{-1}. The critical amorphization fluence (F_c) was defined as the fluence at which all of the diffraction maxima in the selected-area electron diffraction (SAED) pattern had disappeared. A number of different grains with the pyrochlore structure were monitored during the ion irradiations, and final doses were obtained by averaging the experimental data from these grains. The microstructural evolution of actinide-doped pyrochlores were characterized in detail by *ex situ* HRTEM observations using a JEOL 2010 analytical TEM operated at the accelerating voltage of 200 kV.

3. Results and discussion

3.1. Ion beam-induced amorphization and temperature dependence

The microstructural evolution of actinide-doped pyrochlores upon 1 MeV Kr^{2+} irradiation at different ion fluences has been followed in detail by monitoring the SAED patterns (Figs. 1–3). All of the titanate pyrochlores are sensitive to ion beam-induced amorphization at room temperature. The critical amorphization fluences at room temperature for $Ca_{1.04}Ce_{0.97}Ti_{1.99}O_{6.96}$, $(Ca_{0.62}Gd_{0.97}U_{0.23})(Zr_{0.84}Ti_{1.34})O_{6.90}$, and $(Ca_{0.47}Gd_{0.95}Th_{0.40})(Zr_{1.29}Ti_{0.89})O_{7.05}$ upon 1 MeV Kr^{2+} irradiation are 2.0, 3.75 and 5.62×10^{14} ions/cm^2, respectively. For pure zirconate pyrochlores, $(Ca_{0.44}GdTh_{0.42})Zr_{2.13}O_{7.05}$ and $Ca_{0.91}Th_{0.84}Zr_{2.25}O_{7.09}$, amorphization could not be achieved at 25 K at a fluence of 1.06×10^{15} ions/cm^2 (Fig. 4). These results are consistent with the previous study in which the radiation resistance of $Gd_2(Ti_{1-x}Zr_x)_2O_7$ increases as the concentration of Zr increases, and the end member zirconate pyrochlore (e.g., $Gd_2Zr_2O_7$) is highly radiation resistant [9]. Fig. 5 shows the temperature dependence of the actinide-doped pyrochlores to ion beam-induced amorphization. The critical amorphization fluence increases with increasing temperature due to dynamic annealing effects. Above a critical temperature, T_c, the critical amorphization fluence increases to infinity, and complete amorphization does not occur. The critical amorphization temperatures of

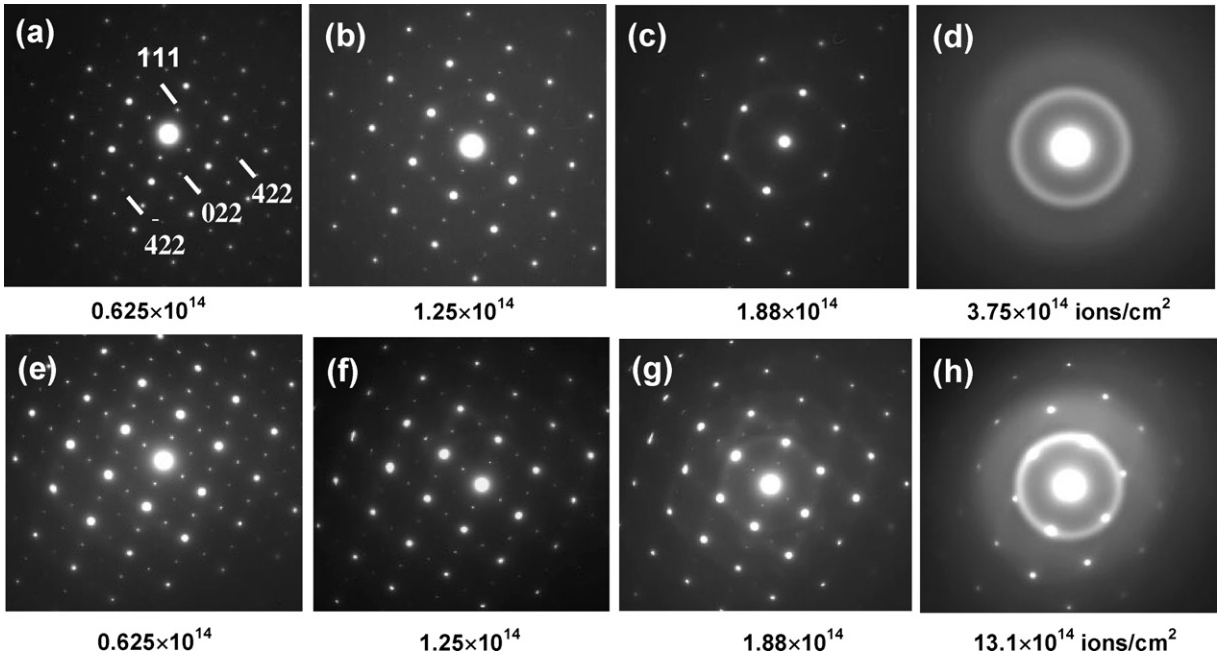

Fig. 2. SAED patterns of $(Ca_{0.62}Gd_{0.97}U_{0.23})(Zr_{0.84}Ti_{1.34})O_{6.90}$ irradiated by 1 MeV Kr^{2+} at room temperature (upper row) and 798 K (lower row).

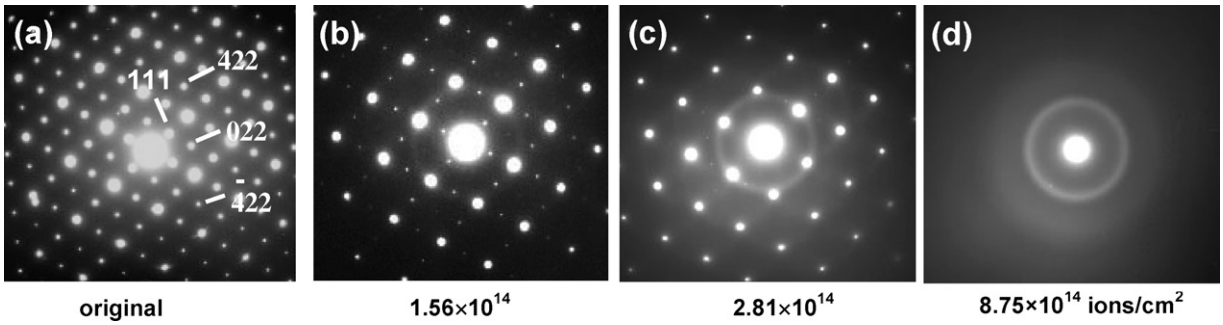

Fig. 3. SAED patterns of $(Ca_{0.47}Gd_{0.95}Th_{0.40})(Zr_{1.29}Ti_{0.89})O_{7.05}$ irradiated by 1 MeV Kr^{2+} at 473 K at different ion fluences: (a) original; (b) 1.56; (c) 2.81; (d) 8.75×10^{14} ions/cm^2.

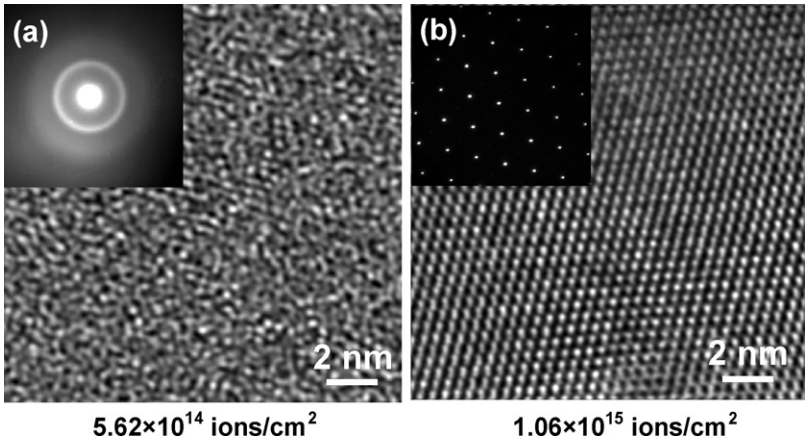

Fig. 4. High-resolution TEM images and corresponding SAED patterns of (a) $(Ca_{0.47}Gd_{0.95}Th_{0.40})(Zr_{1.29}Ti_{0.89})O_{7.05}$ and (b) $(Ca_{0.44}GdTh_{0.42})Zr_{2.13}O_{7.05}$ irradiated by 1 MeV Kr^{2+} at room temperature and 25 K, respectively.

$Ca_{1.04}Ce_{0.97}Ti_{1.99}O_{6.96}$, $(Ca_{0.62}Gd_{0.97}U_{0.23})(Zr_{0.84}Ti_{1.34})O_{6.90}$, and $(Ca_{0.47}Gd_{0.95}Th_{0.40})(Zr_{1.29}Ti_{0.89})O_{7.05}$ are ~1060, 820 and 550 K, respectively. The lower critical amorphization temperatures for actinide-doped pyrochlores is consistent with the higher critical amorphization fluences for Zr-rich compositions at room temperature.

The critical amorphization temperatures of actinide-doped pyrochlores can be compared to data for the solid-solution binary, Gd_2-$Ti_{2-x}Zr_x$-O_7, upon 1 MeV Kr^{2+} ion irradiation (Fig. 6). A close correlation between the critical amorphization temperature and average cation ionic radius ratio is demonstrated. These results are also consistent with recent systematic ion beam irradiation studies on a series of titanate pyrochlores $A_2Ti_2O_7$ (A = Lu to Sm, and Y) [10], zirconate pyrochlores $A_2Zr_2O_7$ (A = Gd, Eu, Sm and La) [11] and stannate pyrochlores [15]. Generally, the "radiation resistance" of pyrochlores is

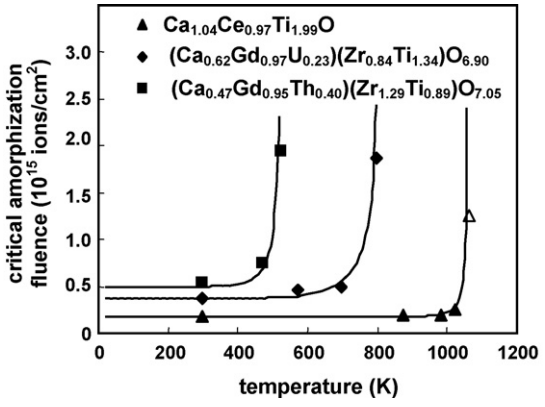

Fig. 5. Critical amorphization fluences of actinide-doped pyrochlores vs. irradiation temperature.

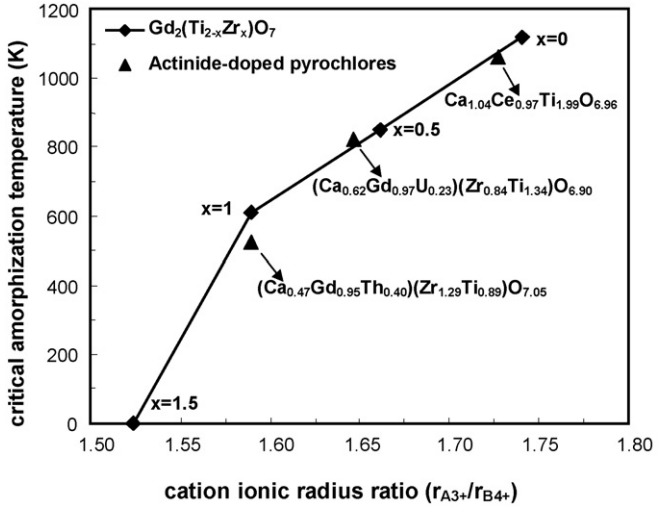

Fig. 6. Critical amorphization temperatures of actinide-doped pyrochlores as a function of average cation ionic radius ratio ($r_{A^{3+}}/r_{B^{4+}}$). The data of $Gd_2(Ti_{2-x}Zr_x)O_7$ are included for comparison [9].

closely related to the cation ionic radius ratio and x positional parameter for the 48f oxygen (the only atom in the structure that does not occupy a special position). A decrease in the average ionic radius ratio of the A- and B-sites (r_A/r_B) generally leads to a decrease in the critical temperature for amorphization. The lower the critical temperature for amorphization the more the phase is considered to be "resistant" to radiation damage because the radiation damage anneals at relatively lower temperatures. In the case of zirconate pyrochlores, the radiation-induced transformation is to a defect fluorite structure (the resulting of cation and anion disordering of the pyrochlore structure) rather than the aperiodic state [9].

3.2. Order–disorder structural transition

In addition to ion beam-induced amorphization, a pyrochlore-to-fluorite structural transition occurred for all of the compositions, as evidenced by the strong diffraction maxima of the fluorite unit cell observed in the SAED patterns with increasing ion fluences (Figs. 2c and 3c). The order–disorder structural transition results from the disordering of cation and anion sublattices upon ion beam irradiation. For $Ca_{1.04}Ce_{0.97}Ti_{1.99}O_{6.96}$, the pyrochlore-to-fluorite structural transition occurred simultaneously with the amorphization process, similar to that observed for other titanate pyrochlores (e.g., $Gd_2Ti_2O_7$) [9,18]. For the Zr-rich compositions, the ion beam-induced pyrochlore-to-fluorite structural transition occurred prior to the amorphization process. The pyrochlore structure is a unique oxide in that the disordering processes can occur independently on both the anion and cation sublattices [19]. A detailed *in situ* study of the order–disorder transition in ion irradiated titanate pyrochlores has shown that anion disordering precedes the disordering of the cations, and upon ion irradiation, an anion-disordered pyrochlore can form with significant anion disordering, while still retaining substantial cation order [13,20]. This anion-disordered pyrochlore is also observed in all of the actinide-doped pyrochlores upon ion irradiation, as shown by the disappearance of characteristic diffraction maxima ($h+k+l=4n$, for which individual indices are not a multiple of 4) corresponding to the anion order [21] in the selected-area electron diffraction pattern (Figs. 2b and f and 3b).

Chemical composition and irradiation temperature appear to have no significant effects on the anion-disordering process. The ion fluence driving the disordering of the anion sublattices has been determined to occur in the range of $(1.25\sim1.50)\times10^{14}$ ions/cm^2 (Figs. 2b and 3b). Anion disordering is almost completed at an ion fluence of 1.25×10^{14} ions/cm^2 for $(Ca_{0.62}Gd_{0.97}U_{0.23})(Zr_{0.84}Ti_{1.34})O_{6.90}$ irradiated at 798 K (Fig. 2f), similar to that observed at room temperature, despite the fact that complete amorphization cannot be achieved at this temperature. However, significant cation ordering is retained for $(Ca_{0.62}Gd_{0.97}U_{0.23})(Zr_{0.84}Ti_{1.34})O_{6.90}$ irradiated at 798 K to a fluence of 1.88×10^{14} ions/cm^2, at which a complete disordering of A- and B-site cations occurs at room temperature (Fig. 2c). In the case of $(Ca_{0.47}Gd_{0.95}Th_{0.40})(Zr_{1.29}Ti_{0.89})O_{7.05}$, complete cation disordering does not occur at a fluence of 2.81×10^{14} ions/cm^2 (Fig. 3c). These results suggest that the ion beam-induced anion disordering is almost temperature independent; while, cation disordering is more sensitive to the change in the chemical composition and irradiation temperature. A molecular dynamic simulation of 6 keV U^{4+} in $La_2Zr_2O_7$ has indicated that a significantly larger number of oxygen atoms are displaced from their equilibrium positions than are the La and Zr during the displacement cascade formation at $t=0.3$ ps. Within several picoseconds ($\sim$7.5 ps), more than 90% of the displaced anions and cations return to their initial positions or occupy equivalent crystallographic sites [22]. Thus, this defect recovery process, due to dynamic annealing, leads to a significant anion disordering, but cation ordering may be retained. Specifically, the ease of the rearrangement of oxygen atoms displaced from 48f position to the unoccupied 8a position makes the anion-disordering process more energetically favorable and less temperature and composition dependent.

4. Conclusions

Samples of actinide- and Ce-doped pyrochlores including: $Ca_{1.04}Ce_{0.97}Ti_{1.99}O_{6.96}$, $(Ca_{0.62}Gd_{0.97}U_{0.23})(Zr_{0.84}Ti_{1.34})O_{6.90}$, $(Ca_{0.47}Gd_{0.95}Th_{0.40})(Zr_{1.29}Ti_{0.89})O_{7.05}$, $(Ca_{0.44}GdTh_{0.42})Zr_{2.13}O_{7.05}$ and $Ca_{0.91}Th_{0.84}Zr_{2.25}O_{7.09}$, have been irradiated by 1 MeV Kr^{2+} in the temperature range of 25–1100 K. An ion beam-induced pyrochlore-to-fluorite structural transition occurred for all of actinide-doped compositions, and an anion-disordered pyrochlore was created prior to the transformation of the pyrochlore structure to the defect-fluorite structure-type. Anion disordering was found to be essentially independent of composition and irradiation temperature. The critical amorphization fluence increases with increasing Zr-content in the pyrochlore structure. The critical amorphization temperatures of $Ca_{1.04}Ce_{0.97}Ti_{1.99}O_{6.96}$, $(Ca_{0.62}Gd_{0.97}U_{0.23})(Zr_{0.84}Ti_{1.34})O_{6.90}$, $(Ca_{0.47}Gd_{0.95}Th_{0.40})(Zr_{1.29}Ti_{0.89})O_{7.05}$ upon 1 MeV Kr^{2+} irradiation are $\sim$1060, 820 and 550 K, respectively. No ion beam-induced amorphization has been observed for the Zr-rich compositions of $(Ca_{0.44}GdTh_{0.42})Zr_{2.13}O_{7.05}$ and $Ca_{0.91}Th_{0.84}Zr_{2.25}O_{7.09}$ at 25 K. A close correlation between the critical amorphization temperature of actinide-doped pyrochlores and the average ionic radius ratio at the A- and B-sites was observed. These results suggest that complex pyrochlore compositions, those with high concentrations of actinides and lanthanides, exhibit a wide range of responses to radiation: amorphization or disordering to the defect fluorite structure. The results of these systematic studies of radiation-response allow one to design actinide-bearing waste forms that will have a predictable response to radiation as a function of a specific composition and temperature. These ion beam irradiation data, however, must be confirmed by actinide-doping experiments (e.g., ^{238}Pu or ^{244}Cm) to equivalent fluences as attained in the ion beam irradiation experiments.

Acknowledgements

We are grateful to the staff of the IVEM-Tandem Facility at the Argonne National Laboratory for assistance during ion beam irradiation experiments. This work was supported by the Office

of Basic Energy Sciences, U.S. Department of Energy under DOE grants DE-FG02-97ER45656 and DE-FG02-04ER15582.

References

[1] R.C. Ewing, W.J. Weber, J. Lian, J. Appl. Phys. 95 (2004) 5949.
[2] K.E. Sickafus, L. Minervini, R.W. Grimes, J.A. Valdez, M. Ishimaru, F. Li, K.J. McClellan, T. Hartmann, Science 289 (2000) 748.
[3] W.J. Weber, R.C. Ewing, Science 289 (2000) 2051.
[4] K.B. Helean, A. Navrotsky, E.R. Vance, M.L. Carter, B. Ebbinghaus, O. Krikorian, J. Lian, L.M. Wang, J.G. Catalano, J. Nucl. Mater. 303 (2002) 226.
[5] J. Lian, L.M. Wang, S.X. Wang, J. Chen, L.A. Boatner, R.C. Ewing, Phys. Rev. Lett. 87 (2001) 145901.
[6] A.A. Digeos, J.A. Valdez, K.E. Sickafus, S. Atio, R.W. Grimes, A.R. Boccaccini, J. Mater. Sci. 38 (2003) 1597.
[7] S.S. Shoup, C.E. Bamberger, R.G. Haire, J. Am. Ceram. Soc. 79 (1996) 1489.
[8] R.E. Sykora, P.E. Raison, R.G. Haire, J. Solid State Chem. 178 (2005) 578.
[9] S.X. Wang, B.D. Begg, L.M. Wang, R.C. Ewing, W.J. Weber, K.V.G. Kutty, J. Mater. Res. 14 (1999) 4470.
[10] J. Lian, J. Chen, L.M. Wang, R.C. Ewing, J.M. Farmer, L.A. Boatner, K.B. Helean, Phys. Rev. B 68 (2003) 134107.
[11] J. Lian, X.T. Zu, K.V.G. Kutty, J. Chen, L.M. Wang, R.C. Ewing, Phys. Rev. B 66 (2002) 054108.
[12] B.D. Begg, N.J. Hess, W.J. Weber, R. Devanathan, J.P. Icenhower, S. Thevuthasan, B.P. McGrail, J. Nucl. Mater. 288 (2001) 208.
[13] J. Lian, L.M. Wang, R.G. Haire, K.B. Helean, R.C. Ewing, Nucl. Instrum. Meth. Phys. Res. B 218 (2004) 236.
[14] J. Lian, R.C. Ewing, L.M. Wang, K.B. Helean, J. Mater. Res. 19 (2004) 1575.
[15] J. Lian, K.B. Helean, B.J. Kennedy, L.M. Wang, A. Navrotsky, R.C. Ewing, J. Phys. Chem. B 110 (2006) 2343.
[16] W.J. Weber, J.W. Wald, Hj. Matzke, Mater. Lett. 3 (1985) 173.
[17] N.P. Laverov, S.V. Yudintsev, S.V. Stefanovsky, Y.N. Jang, R.C. Ewing, Mat. Res. Soc. Symp. Proc. 713 (2002) 337.
[18] S.X. Wang, L.M. Wang, R.C. Ewing, G.S. Was, G.R. Lumpkin, Nucl. Instrum. Meth. Phys. Res. B 148 (1999) 704.
[19] B.J. Wuensch, K.W. Eberman, JOM 52 (2000) 19.
[20] J. Lian, L. Wang, J. Chen, K. Sun, R.C. Ewing, J.M. Farmer, L.A. Boatner, Acta Mater. 51 (2003) 1493.
[21] T. Hahn (Ed.), International Tables for Crystallography, 4th ed., Kluwer, 1996, 686.
[22] A. Chartier, C. Meis, J.P. Crocombette, L.R. Corrales, W.J. Weber, Phys. Rev. B 67 (2003) 174102.